Determination of Base Stresses in Rectangular Footings under Biaxial Bending[†]

Günay ÖZMEN*

ABSTRACT

All the footings of buildings in seismic regions are to be designed according to biaxial bending moments. The purpose of this paper is to develop a general method for calculating the base pressures of rectangular footings under biaxial bending. First the footings which are exposed to large eccentricity are classified according to the shape of the pressure region. Then the formulation given by Löser for the design of rectangular columns subjected to biaxial bending are generalized and applied to the calculation of base stresses. Since the position of the neutral axis is not known initially, a process of successive approximations is developed. The application of the computation procedure is demonstrated on a numerical example.

Keywords: *Biaxial bending, single footings, base pressures, successive approximations.*

1. INTRODUCTION

It may be considered both safe and economic to provide an individual foundation for each column, in cases when the bearing capacity of the foundation soil is sufficiently high or the loads are comparatively low. These individual foundations which are called "Footings" are generally constructed rectangular in shape, [1], [2], [3], [4], [5]. As a special case, the schematic elevation of a rectangular footing under the effect of vertical load V and uni-directional bending moment M_y is shown in Figure 1.
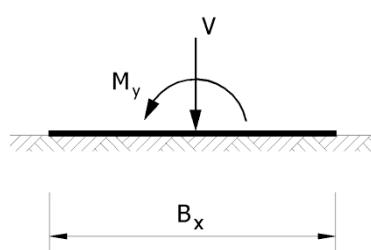
Figure 1: *Footing under the effect of uni-directional moment*

* Istanbul Technical University, (Retired), Istanbul, Turkey - gunozmen@yahoo.com

The dimensions of the footing are $B_x \times B_y$. The base stresses for this kind of footings are readily computed by using the well known formulae of strength of materials. The eccentricity e of the vertical load is defined as

$$e = \frac{M_y}{V} \ . \tag{1}$$

However, when the vertical load is situated outside of the region which is called the "Core", i.e. when

$$e > B_x \ / \ 6 \tag{2}$$

an unstressed zone develops at the base of the footing. This special state is named "Large Eccentricity" and the corresponding stress distribution is as shown in Figure 2.
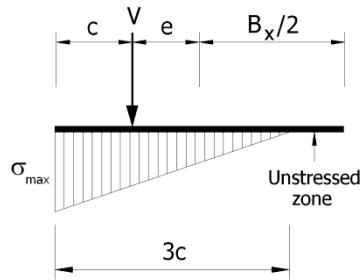
Figure 2*: Stress distribution for large eccentricity*

In this case, maximum base pressure is computed by

$$\sigma_{max} = 2\frac{V}{3cB_y} = \frac{4}{3}\frac{V}{B_y(B_x - 2e)} \ . \tag{3}$$

2. FOOTINGS UNDER BIAXIAL BENDING

In the Turkish Earthquake Code which is valid since 2007, it is required that the interaction of the two orthogonal excitation directions is to be taken into account, [6]. Hence, in seismic regions it is necessary to design all the columns (and foundations) of the buildings to be under the effect of biaxial bending.

Computation of the base stresses of the footings under biaxial bending moments is a rather complex task except certain special cases. This subject is investigated in a rather comprehensive and detailed manner by Köseoğlu and extensive explanations are presented,

[1]. For triangular and trapezoidal pressure zones exact formulae are given while the formulae for pentagonal zones are approximate. Trupia and Saygun have also developed exact formulae for triangular and trapezoidal pressure zones and presented a design chart for pentagonal zones, [5].

The purpose of this study is to develop a base stress computation method which is independent of the shape of the pressure zone, i.e. valid for triangular, trapezoidal and pentagonal zone shapes. To begin with, the explanations given by Köseoğlu will be summarized and discussed.

Schematic stress distribution of a rectangular footing under the effect of biaxial bending together with vertical load is shown in Figure 3.
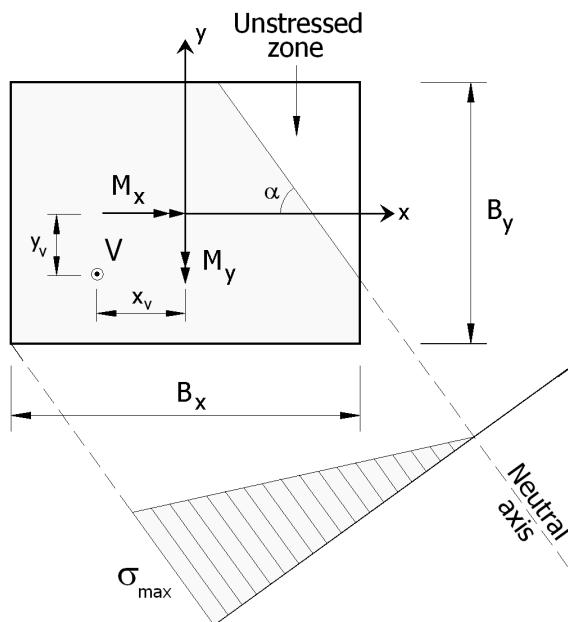
Figure 3: Loading at footing base and stress distribution

Compression zone is shown as shaded on the figure. It is assumed that the load V is acting vertical to the paper surface at the centroid of the rectangular area. The sign convention for the load is taken positive in downward direction. In the cases where the related column is situated at a different location than the centroid, the forces acting on the footing can be transferred to the centroid and the formulae given below can be applied without modification. Positive directions for the bending moments M_x and M_y are so chosen that the maximum base stress occurs at the lower left corner of the footing base. The coordinates of the application point of the vertical load V are

$$x_v = -\frac{M_y}{V} \qquad\qquad y_v = -\frac{M_x}{V} \ . \tag{4}$$

both of which are negative according to the chosen sign conventions. The angle between the neutral axis and axis x is denoted by α.

The neutral axis may exist in various locations and inclinations depending on the values of V, M_x, M_y and the footing dimensions B_x, B_y. An "Unstressed Zone" in a variety of shapes and sizes may occur according to the position of the neutral axis. It may be shown that the shape and size of the compression zone depends on the application point of the vertical load V. The base of the footing may be considered as being separated into 13 regions according to the shape of the compression zone. These regions may be collected in 5 groups, as shown in Figure 4, giving the same number to the regions of the same character.
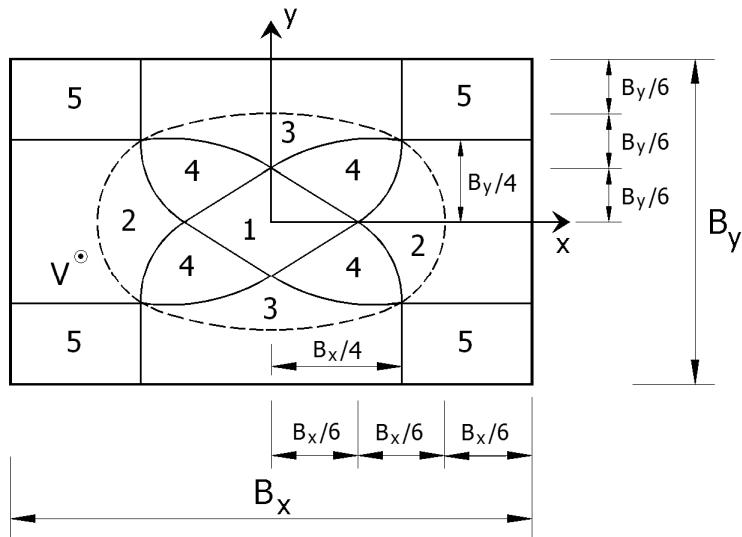
***Figure 4**: Footing base regions according to compression zone shapes*

The compression zone types corresponding to these regions are shown in Figure 5.

Compression zones are shown as shaded in the figure. Symmetric shapes with respect to x and/or y axes may also occur due to the axes of symmetry. In the following, characteristics are summarized for various types and stress computation formulae are presented.
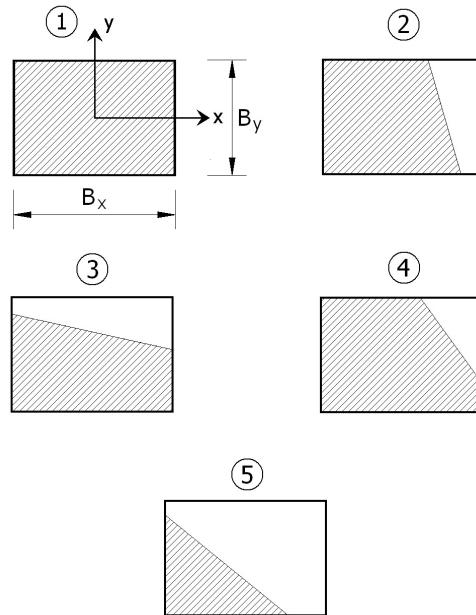
Figure 5*: Compression zone types*

Type 1:

When the application point of the vertical load V remains in the rhombus shaped region, i.e. core, which is denoted as 1 in Figure 4, all the footing base is under compression. In this case, which is called "Small Eccentricity", stresses at all corners can be computed by the well known formula

$$\sigma = \frac{V}{F} \mp \frac{M_x B_y}{2I_x} \mp \frac{M_y B_x}{2I_y} \qquad (5)$$

where F, I_x and I_y, are the base area and moments of inertia around axes x and y, respectively.

Type 2:

When the application point of vertical load V is within the regions indicated with 2 in Figure 4, "Large eccentricity" takes place where a trapezoidal shaped unstressed zone occurs. In this case, the compression zone is also trapezoidal as shown in Figure 5 and the maximum corner stress may be computed by using the formulae given in [1], i.e. by

$$t_y = \frac{B_y}{12}\left(-\frac{B_y}{y_v} + \sqrt{\left(\frac{B_y}{y_v}\right)^2 - 12}\right) \quad ; \quad tg\alpha = \frac{3}{2}\frac{B_x + 2x_v}{t_y - y_v} \tag{6}$$

$$\sigma_{max} = \frac{12V}{B_y tg\alpha}\frac{B_y + 2t_y}{B_y^2 + 12t_y^2} . \tag{7}$$

Type 3:

When the application point of vertical load V is within the regions denoted as 3 in Figure 4, large eccentricity is again the case where trapezoidal shapes prevail for both the compression and unstressed zones, Figure 5. In this case the maximum corner stress may also be computed by using the formulae given in [1], i.e. by

$$t_x = \frac{B_x}{12}\left(-\frac{B_x}{x_v} + \sqrt{\left(\frac{B_x}{x_v}\right)^2 - 12}\right) \quad ; \quad tg\alpha = \frac{3}{2}\frac{B_y + 2y_v}{t_x - x_v} \tag{8}$$

$$\sigma_{max} = \frac{12V}{B_x tg\alpha}\frac{B_x + 2t_x}{B_x^2 + 12t_x^2} . \tag{9}$$

Type 4:

When the application point of vertical load V is within the regions denoted as 4 in Figure 4, large eccentricity takes place as well. In this case the compression and the unstressed zones are pentagonal and triangular, respectively, Figure 5. Exact computation of the corner stresses proves to be rather complex for this type of stress distribution. However, approximate formulae which may be considered adequate for practical applications are presented in [1] as follows:

$$\varepsilon = \frac{|x_v|}{B_x} + \frac{|y_v|}{B_y} \tag{10}$$

$$\sigma_{max} = \frac{\varepsilon V}{B_x B_y}\left[12 - 3.9(6\varepsilon - 1)(1 - 2\varepsilon)(2.3 - 2\varepsilon)\right]. \tag{11}$$

Type 5:

The oval region encircled by a dashed line in Figure 4 is called the "Secondary Core" which contains whole of the regions 1 and 4 and certain parts of the regions 2 and 3. When the application point of vertical load V is outside of the secondary core, "Excessive large eccentricity" occurs. This case where the compression zone is smaller then the unstressed zone should not be preferred in application. It is stated that, this type of stress distribution is not allowed by some of the design codes, [1], [7]. The regions shown as 5 remain wholly outside of the secondary core. In these regions, the triangular compression zones are smaller than the pentagonal unstressed zones. Stress computation formulae for this type do not exist in the references.

In this study, a method for base stress computation for the case of large eccentricity is developed. The presented method is general, i.e. independent of the shape of the pressure zone.

3. CROSS SECTION CHARACTERISTICS OF THE PRESSURE ZONE

The section characteristics of the pressure zone should be determined prior to stress calculations. A footing base with pentagonal pressure zone is shown in Figure 6. This type of pressure zone may be considered general, i.e. covering all the other types as special cases, as will be explained shortly.
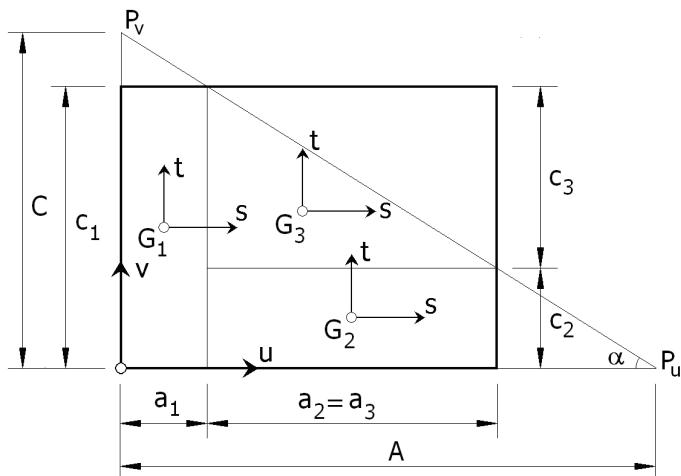
Figure 6: *Footing base and pressure zone parts*

Intersection points of the neutral axis with the axes u and v are denoted by P_u and P_v, respectively. The respective distances of these points to the lower left point of the base are designated as A and C. These quantities will be used as main variables in stress calculations. In order to obtain the section characteristics, the pressure zone is divided into

three parts consisting of two rectangular and one triangular region. The dimensions a_1, c_1, a_2, c_2, a_3 and c_3 can be calculated easily by using the values B_x, B_y, A and C. The conditions related to the various pressure zone types and the dimensions of the section parts for these types are shown in Tables 1 and 2, respectively.

Table 1: *Conditions for pressure zone types*

Type	Condition
1	$A > B_x$ & $C > B_y$ & $\dfrac{B_x}{A} + \dfrac{B_y}{C} < 1$
2	$A < B_x$ & $C > B_y$
3	$A > B_x$ & $C < B_y$
4	$A > B_x$ & $C > B_y$ & $\dfrac{B_x}{A} + \dfrac{B_y}{C} > 1$
5	$A < B_x$ & $C < B_y$

Table 2: *Dimensions of pressure zone parts*

Type	a_1	c_1	a_2	c_2	a_3	c_3
1	B_x	B_y	0	0	0	0
2	$(C-B_y)/tg\alpha$	B_y	0	0	$A-a_1$	B_y
3	0	0	B_x	$(A-B_x)\,tg\alpha$	B_x	$C-c_2$
4	$(C-B_y)/tg\alpha$	B_y	B_x-a_1	$(A-B_x)\,tg\alpha$	B_x-a_1	c_2
5	0	0	0	0	A	C

As can be seen in Table 2, all dimensions a_i and c_i are nonzero for only Type 4. Hence this pressure zone type can be considered general covering all the other types as special cases. For each part, coordinates u_g, v_g of the individual centroids G_1, G_2, G_3 with respect to the axes u and v, areas F and moments of inertia I_s, I_t and I_{st} with respect to the individual axes s,t are shown in Table 3.

Table 3*: Section Characteristics of pressure zone parts*

	Rectangular part (1)	Rectangular part (2)	Triangular part (3)
u_g	$\dfrac{1}{2}a_1$	$a_1 + \dfrac{1}{2}a_2$	$a_1 + \dfrac{1}{3}a_3$
v_g	$\dfrac{1}{2}c_1$	$\dfrac{1}{2}c_2$	$c_2 + \dfrac{1}{3}c_3$
F	$a_1 c_1$	$a_2 c_2$	$\dfrac{1}{2}a_3 c_3$
I_s	$\dfrac{a_1 c_1^3}{12}$	$\dfrac{a_2 c_2^3}{12}$	$\dfrac{a_3 c_3^3}{36}$
I_t	$\dfrac{a_1^3 c_1}{12}$	$\dfrac{a_2^3 c_2}{12}$	$\dfrac{a_3^3 c_3}{36}$
I_{st}	0	0	$-\dfrac{a_3^2 c_3^2}{72}$

Area F and the coordinates u_g and v_g of the centroid G for the whole pressure zone are computed by

$$F = \sum_{i=1}^{3} F_i \tag{12}$$

$$u_g = \frac{\sum_{i=1}^{3} u_{g,i} F_i}{F} \tag{13}$$

$$v_g = \frac{\sum_{i=1}^{3} v_{g,i} F_i}{F} . \tag{14}$$

Moments of inertia with respect to the axes $\bar{x}$ and $\bar{y}$ passing through the centroid G can be expressed by

$$I_x = \sum_{i=1}^{3} I_{s,i} + \sum_{i=1}^{3} F_i f_i^2 \tag{15}$$

$$I_y = \sum_{i=1}^{3} I_{t,i} + \sum_{i=1}^{3} F_i e_i^2 \qquad (16)$$

$$I_{xy} = \sum_{i=1}^{3} I_{st,i} + \sum_{i=1}^{3} F_i e_i f_i \qquad (17)$$

where e_i and f_i denote the distances of pressure zone parts' centroids to the centroid G, Figure 7.
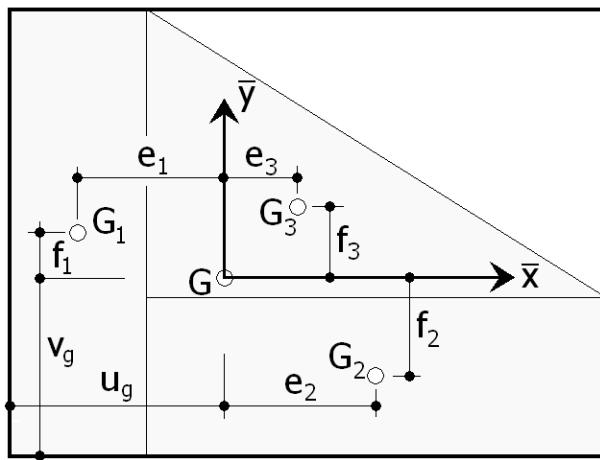
Figure 7: *Distances of pressure zone parts' centroids*

4. COMPUTATION OF STRESSES

For many years, the book known as "Löser" has been one of the main sources of reference in reinforced concrete for structural engineers, [8]. This book includes extensive and detailed information on the design of RC structural elements according to the elastic theory. Nowadays a considerable portion of the information included in this book is outdated due to the usage of the "Ultimate Strength" theory in designing RC structural elements. However, it is seen that the formulae included in the section named "Rectangular cross sections subjected to biaxial bending moments" in this book can be used for computation of stresses in footings under biaxial bending. As a matter of fact, if the contribution of reinforcement is removed from the said formulae, the remaining parts consist of the computation of concrete stresses and can be used for determining base stresses of footings. Moreover, when the above given expressions for moments of inertia are used in the Löser formulae, stress computation procedure will be generalized including pentagonal pressure zones. The generalized stress computation procedure for footings will be explained in the following pages.

The coordinates x_v, y_v of the application point of the vertical load V were given by Eqs. (4). The coordinates of this point with respect to axes $\overline{x}$ and $\overline{y}$ passing through the centroid of the compression zone are

$$\overline{x}_v = x_v + \frac{B_x}{2} - u_g \quad ; \quad \overline{y}_v = y_v + \frac{B_y}{2} - v_g , \tag{18}$$
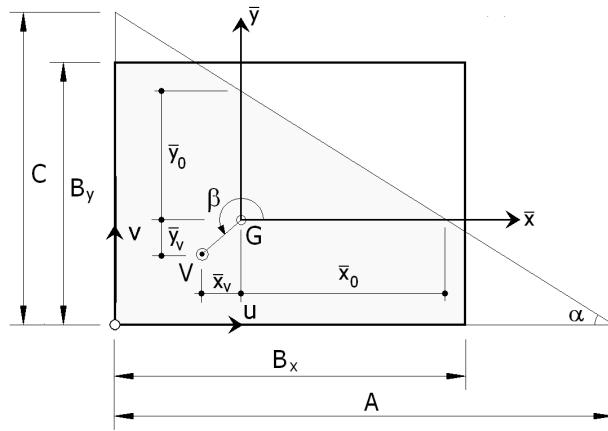
Figure 8*: Auxiliary variables for stress computations*

If the angle between the vector GV and horizontal axis $\overline{x}$ is denoted by β, then

$$tg\beta = \frac{\overline{y}_v}{\overline{x}_v} \tag{19}$$

and the slope of the neutral axis can be computed by

$$tg\alpha = \frac{I_x - I_{xy} tg\beta}{I_y tg\beta - I_{xy}} , \tag{20}$$

In Figure 8, [8]. The distances of the points of intersection of the neutral axis with axes $\overline{x}$ and $\overline{y}$ to point G are

$$\overline{x}_0 = -\frac{I_y + I_{xy}/tg\alpha}{\overline{x}_v F} \quad ; \quad \overline{y}_0 = \overline{x}_0 tg\alpha , \tag{21}$$

respectively. The distances of the points of intersection of the neutral axis with axes u and v to the lower left point can be expressed by

$$A = u_g + \bar{x}_0 + y_g / tg\alpha \quad ; \quad C = y_g + \bar{y}_0 + u_g tg\alpha , \tag{22}$$

respectively, as in Figure 8.

Then the base stress at any point with coordinates $\bar{x}$ and $\bar{y}$ is computed by

$$\sigma = \frac{V}{F} \left(\frac{\bar{x} tg\alpha + \bar{y}}{\bar{y}_0} - 1 \right) \tag{23}$$

and the maximum base stress at lower left point by

$$\sigma_{max} = \frac{AV}{\bar{x}_0 F} , \tag{24}$$

[8].

5. COMPUTATION PROCEDURE

As explained in the preceding section, in order to compute the auxiliary variables $\bar{x}_v$, $\bar{y}_v$, $tg\beta$, $tg\alpha$, $\bar{x}_0$ and $\bar{y}_0$, the "Cross Section Characteristics" of the pressure zone are needed. But all the sectional characteristics are dependent on the main variables A and C except for the small eccentricity case, i.e. Type 1, which can be seen by inspecting Tables 2 and 3. For the cases of large eccentricity, a successive approximation method should be applied, since the values of A and C are not known initially. Computation procedure can be outlined as follows:

1. Firstly, all corner stresses are calculated by using Eq. (5). If all the corner stresses are positive (compression) then small eccentricity is the case and stress computation is completed.

2. If at least one of the corner stresses is found to be negative (tension), than large eccentricity will occur. In this case successive approximation is started by choosing proper initial values for A and C.

3. The conditions in Table 1 are inspected by using the chosen A and C values and the type of the compression zone is determined.

4. The dimensions and cross sectional characteristics of the compression zone parts are computed by using the formulae given in Tables 2 and 3, respectively.

5. The cross sectional characteristics for the whole of the compression zone are computed by using Eqs. (12) ~ (17).

6. Auxiliary variables and new values for A and C are computed by using Eqs. (18) ~ (21) and (22), respectively.

7. If the new values of A and C are not sufficiently close to the previous values, steps 3 ~ 6 are repeated.

8. When the new values of A and C are sufficiently close to the previous values, successive approximation procedure is terminated and corner stresses are computed by means of Eq. (23).

This procedure is quickly convergent and the values of corner stresses are not highly sensitive to the variations in the values of A and C. Numerical applications have shown that, step numbers are not very much dependent on the chosen initial values of A and C. It can be said that, the most appropriate initial values for A and C are the values obtained by simple proportioning using the initial stress values computed by Eq. (5).

6. NUMERICAL APPLICATION

A rectangular footing whose dimensions are $B_x = 2.50$ m and $B_y = 1.50$ m is under the effect of a vertical load of $V = 400$ kN together with bending moments $M_x = 120$ kNm and $M_y = 150$ kNm. Corner stresses found by using Eq. (5) are shown in Table 4.

Table 4: Initial corner stresses

Corner	σ (kPa)
Lower left	330.7
Upper left	74.7
Upper right	−117.3
Lower right	138.7

Since the stress at upper right corner is negative (tension) large eccentricity is the case; hence successive approximations should be applied. Initial values for A and C are computed by simple proportioning using the above corner stresses yielding

A = 4.306 m ;   C = 1.938 m.

If the conditions in Table 1 are inspected by using these values it is seen that

$$A > B_x \quad ; \quad C > B_y \quad ; \quad \frac{B_x}{A} + \frac{B_y}{C} > 1 \, ,$$

i.e. the compression zone is pentagonal, (Type 4). By using the relevant formulae in Tables 2 and 3, dimensions and cross section characteristics of the compression zone parts are computed. Then moments of inertia of the whole compression zone are obtained as

$I_x = 0.5237$ m^4

$I_y = 1.5499$ m^4

$I_{xy} = -0.2203$ m^4

by using Eqs. (12) ~ (17). The auxiliary variables are computed by means of these values and Eqs. (18) ~ (21) which yield the new values for A and C as

A = 3.874 m ;   C = 1.796 m

through Eqs. (22). Since these values are not sufficiently close to the initial values it is necessary to continue successive approximations. The results of successive steps are shown in Table 5.

Table 5: Results of successive steps

Step	A (m)	C (m)	σ_{max} (kPa)
1	4.306	1.938	330.7
2	3.874	1.796	366.8
3	3.807	1.768	373.1
4	3.804	1.767	373.3

It is seen that the results of 4th step are sufficiently close to those of 3rd step. Hence the successive approximations is terminated and final corner stresses are computed by Eq. (23) which are shown in Table 6.

Table 6: Final corner stresses

Corner	σ (kPa)
Lower left	373.3
Upper left	56.5
Upper right	–
Lower right	128.0

It is seen that the exact results are obtained in merely 4 steps, i.e. the proposed method is quickly convergent. On the other hand, by using the approximate formula (11) given by Köseoğlu [1] yields

σ_{max} = 373.1 kPa

which has an error of merely – 0.6%. Weighted average error for all the corner stresses is computed as ± 3.7% where the weights are taken as the absolute values of the stresses. Investigations on several numerical examples have revealed that the average errors for Köseoğlu formulae are in the order of ± 5 %; hence they may be considered suitable for practical applications. The chart and formulae given by Trupia and Saygun also give results which are sufficiently accurate.

7. CONCLUSIONS

In this study, a method for base stress computation for rectangular footings under the effect of biaxial loading is developed. The results obtained may be summarized as follows:

1. The method which is developed for the case of large eccentricity is independent of the shape of the compression zone. Namely, it is valid for all types of compression zones including triangular, trapezoidal and pentagonal shapes.

2. The proposed successive approximations procedure is quickly convergent i.e. the results are obtained after a few steps.

3. The proposed method and computation procedure can be easily adapted to computer by using any programming language.

4. Köseoğlu formulae are tested and it is determined that they may be used successfully in practical applications.

Symbols

A:	Abscissa of the intersection point of the neutral axis with the horizontal axis passing through lower left point,
a_1, a_2, a_3:	Horizontal dimensions of pressure zone parts,
B_x:	Dimension of the footing in direction x,
B_y:	Dimension of the footing in direction y,
C:	Ordinate of the intersection point of the neutral axis with the vertical axis passing through lower left point,
c:	Distance to the footing's edge in the case of uni-axial bending,
c_1, c_2, c_3:	Vertical dimensions of pressure zone parts,
e:	Eccentricity in the case of uni-axial bending,

e_1, e_2, e_3:   Horizontal distances of the centroids of pressure zone parts to the general centroid,

F: Area of the footing base (pressure zone),

f_1, f_2, f_3:   Vertical distances of the centroids of pressure zone parts to the general centroid,

I_s, I_t, I_{st}:   Moments of inertia of pressure zone parts,

I_x: Moment of inertia of footing base (pressure zone) with respect to axis x,

I_y: Moment of inertia of footing base (pressure zone) with respect to axis y,

I_{xy}:   Product moment of inertia of footing base (pressure zone),

M_x: Bending moment about axis x,

M_y: Bending moment about axis y,

t_x, t_y: Auxiliary variables,

u_g, v_g: Coordinates of the centroid of pressure zone,

V: Vertical load,

x_v: Abscissa of the application point of the vertical load,

y_v: Ordinate of the application point of the vertical load,

α: Inclination of the neutral axis,

β: Angle between the vector passing through the application point of the vertical load and horizontal axis $\overline{x}$,

ε: Auxiliary coefficient,

σ: Corner stress,

σ_{max}:   Maximum corner (edge) stress.

References

[1] Köseoğlu, S., Foundations – Statics and Construction, Matbaa Teknisyenleri Printing House, Istanbul, 1986, (In Turkish).

[2] Ersoy, U., Reinforced Concrete Floors and Foundations, Evrim Publishing House, Ankara, 1995, (In Turkish).

[3] Celep, Z., Kumbasar, N., Reinforced Concrete Structures, Sema Printing, Istanbul, 1996, (In Turkish).

[4] Aka, İ., Keskinel, F., Çılı, F., Çelik, O. C., Reinforced Concrete, Birsen Publishing House, Istanbul, 2001, (In Turkish).

[5] Trupia, A., Saygun, A. – Reinforced Concrete Shallow Foundations, Nobel Printing & Distribution, Ankara, 2009, (In Turkish).

[6] Specification for Buildings to be Constructed in Seismic Regions, Ministry of Public Works and Settlements, Ankara, March 2007, (In Turkish).

[7] DIN 1054 – 1976, Foundation Ground – Safety Loads of Foundation Ground, Bulletin of Ministry of Public Works and Settlements, No. 81, Ankara, 1984, (In Turkish).

[8] Löser, B., Löser – Bemessungsverfahren, Verlag von Wilhelm Ernst & Sohn, Berlin, 1948.